

Spherically symmetric loop quantum gravity: Schwarzschild spacetimes with a cosmological constant

Esteban Mato^{1,*}, Javier Olmedo^{2,†} and Sahil Saini^{3‡}

¹ *Instituto de Física,
Facultad de Ingeniería (Universidad de la República),
Julio Herrera y Reissig 565,
11300 Montevideo, Uruguay,*

² *Departamento de Física Teórica y del Cosmos,
Universidad de Granada, Granada-18071, Spain.*

³ *Department of Physics,
Guru Jambheshwar University of Science & Technology,
Hisar, Haryana 125001, India*

We provide a quantization of the Schwarzschild spacetime in the presence of a cosmological constant, based on midisuperspace methods developed in the spherically symmetric sector of loop quantum gravity, using in particular the 'improved dynamics' scheme. We include both the deSitter and anti-deSitter cases. We find that the quantization puts a Planckian upper limit on the possible values of a positive cosmological constant similar to the bounds obtained earlier from studies of homogeneous spacetimes with a cosmological constant. Using semiclassical physical states, we obtain the effective metric and demonstrate the causal structure for various cases. Quantum gravity modifications ensure that the singularity is replaced by a transition surface in all the cases, where the curvature invariants approach mass-independent Planckian bounds. Analysis of the effective stress-energy tensor shows that the null energy condition is violated in the vicinity of the transition surface.

I. INTRODUCTION

In recent years, while we are still far from directly observing quantum gravity effects, black holes have become a test bed for various theories of quantum gravity. A successful and theoretically satisfactory resolution of the black hole singularity is the first step towards building confidence in quantum gravity models. In this direction, considerable progress has been made in loop quantum gravity (LQG). It has been found through numerous studies, approaching the problem from different directions, that loop quantization inevitably resolves the singularity replacing it by a transition surface beyond which the spacetime can be extended. Most of the studies are based on the minisuperspace approach used in loop quantum cosmology, where symmetry-reduction leaves only a finite number of degrees of freedom to be loop quantized. For recent developments using this approach, see [1–3].

In case of spherically symmetric spacetimes, an independent program of loop quantization based on the midisuperspace approximation has been developed. The spherically symmetric framework was initially developed in [4–6, 11, 13] where symmetry reduction was carried out and kinematical framework was laid down. A redefinition of the Hamiltonian constraint was carried out to Abelianize the algebra of the Hamiltonian constraint with itself, which allowed the Dirac quantization of the model to be completed in the case of the Schwarzschild black holes [7–9]. The framework has

*Electronic address: emato@fing.edu.uy

†Electronic address: javolmedo@ugr.es

‡Electronic address: sahilssaini@gjust.org

been further extended [19, 20] to implement the improved dynamics scheme developed by Chiou et. al. [18]. In recent years, this approach has been applied to obtain a quantization of the charged black holes [15, 16].

In this manuscript, we extend the program of spherically symmetric loop quantization to Schwarzschild spacetimes with a cosmological constant Λ , where Λ is kept general and allowed to be both positive or negative. Apart from being of interest in their own right, these models provide an opportunity to study quantum black holes in non asymptotically flat spacetimes. We first Abelianize the classical Hamiltonian constraint by suitable coordinate transformations, and then loop quantize the resulting theory along the lines of [7–9]. Following [16, 17, 19], we implement the improved dynamics scheme first proposed by Chiou et. al. in the case of spherically symmetric spacetimes [18]. Implementing two separate improved dynamics conditions allows us to determine various quantization parameters as done in [16].

We find that a consistent quantization requires putting a mass-independent Planckian upper bound on how large a positive cosmological constant can be, as well as a mass and Λ -dependent lower bound on how small the smallest area spheres can be. The mass-independent upper bound on positive Λ obtained by our loop quantization of spherically symmetric spacetimes is of the same order as the one obtained in case of homogeneous spacetimes with a non-vanishing positive Λ [24, 25]. This ensures that the quantum geometry effects limit the curvature in the asymptotic limit, which is proportional to Λ , to Planckian values at most. We show this explicitly in the section on effective geometry. In agreement with the analysis of homogeneous spacetimes with a non-vanishing negative Λ [26], where no upper bound on the magnitude of Λ was necessitated by loop quantization, no bound on the magnitude of negative Λ was warranted by our quantization of the spherically symmetric models. Further, we found that the leading order term in the lower bound on the radius of smallest area spheres agrees with that obtained for the charged black hole [16] as well as the uncharged Schwarzschild black hole studied in [19, 20] in the improved dynamics scheme. In contrast to the charged black hole where the first order corrections due to charge were negative, we found that they were positive in the case of a cosmological constant.

Using semiclassical physical states, we obtain the effective metric containing the lowest order quantum corrections. We find that the effective metric is regular at the centre and the singularity is replaced by a transition surface which links a trapped region with an anti-trapped region. We analyze the causal structure of the resulting spacetimes - all of which are asymptotically deSitter or anti-deSitter. Depending on the value of the cosmological constant, there are four distinct spacetimes - (i) $0 < 9G^2M^2\Lambda < 1$ corresponds to the conventional Schwarzschild-deSitter spacetime, (ii) $9G^2M^2\Lambda > 1$ corresponds to ultramassive spacetimes with a naked singularity at the centre, (iii) $9G^2M^2\Lambda = 1$ is the special case where the black hole horizon overlaps with the cosmological horizon, and (iv) $\Lambda < 0$ corresponds to the anti-deSitter case. The spacetime represented by the effective metric in all cases is a regular extension of the corresponding classical spacetimes beyond the central singularity. The analysis of curvature invariants reveals that quantum effects only become significant when the curvature approaches Planckian values. In particular, we show that for macroscopic black holes, the curvature invariants approach a mass-independent Planckian bound at the transition surface. The analysis of the effective stress-energy tensor also shows a violation of the null energy condition (NEC) in the vicinity of the transition surface, indicating the resolution of the singularity.

The manuscript is organized as follows. In section II, we provide the classical theory of the symmetry-reduced Schwarzschild spacetime with a cosmological constant and obtain an Abelianized Hamiltonian constraint. Section III contains the kinematical details of loop quantization using the improved dynamics scheme. In section IV on physical states and observables we give the conditions that need to be satisfied for a consistent quantization - which yields a Planckian upper bound on positive Λ . In section V, we obtain the effective metric and derive its physical implications,

including the analysis of causal structure and the behavior of curvature invariants. We summarize our findings in section VI. The details of quantum dynamics of the model are contained in an appendix at the end.

We set the Immirzi parameter $\gamma = 1$ as well as $G = 1 = \hbar$.

II. SCHWARCHILD SPACETIME WITH A COSMOLOGICAL CONSTANT: THE CLASSICAL THEORY

The geometrical sector of the theory is described in terms of Ashtekar variables. In spherically symmetric spacetimes, the connection has two gauge invariant components, (K_φ, K_x) , in the radial and transverse directions, and similarly, the densitized triad has also two gauge invariant components (E^φ, E^x) [11]. They form two canonical pairs of field variables and fulfill the Poisson algebra

$$\{K_x(x), E^x(x')\} = G\delta(x - x'), \quad (2.1)$$

$$\{K_\varphi(x), E^\varphi(x')\} = G\delta(x - x'). \quad (2.2)$$

There is no matter content but we will include a cosmological constant Λ . Therefore, our spacetime will not be asymptotically flat, as we will see.

The total reduced Hamiltonian is a combination of constraints

$$H_T = G^{-1} \int dx (NH_{\text{gr}} + N^x H_x), \quad (2.3)$$

where the diffeomorphism and scalar constraints are given by,

$$H_x = E^\varphi K'_\varphi - (E^x)' K_x, \quad (2.4)$$

$$H_{\text{gr}} = \left(\frac{((E^x)')^2}{8\sqrt{|E^x|}E^\varphi} - \frac{E^\varphi}{2\sqrt{|E^x|}} - 2K_\varphi\sqrt{|E^x|}K_x - \frac{E^\varphi K_\varphi^2}{2\sqrt{|E^x|}} - \frac{\sqrt{|E^x|}(E^x)'(E^\varphi)'}{2(E^\varphi)^2} + \frac{\sqrt{|E^x|}(E^x)''}{2E^\varphi} + \sqrt{|E^x|}E^\varphi\frac{\Lambda}{2} \right). \quad (2.5)$$

The corresponding spacetime metric can be written as

$$ds^2 = -(N^2 - N_x N^x) dt^2 + 2N_x dt dx + \frac{(E^\varphi)^2}{|E^x|} dx^2 + |E^x| d\Omega^2, \quad (2.6)$$

where $d\Omega^2 = d\theta^2 + \sin^2\theta d\varphi^2$ being the metric of the unit sphere and $N_x = g_{xx}N^x = \frac{(E^\varphi)^2}{|E^x|}N^x$.

The constraint algebra

$$\{H_x(N_x), H_x(\tilde{N}_x)\} = H_x(N_x\tilde{N}'_x - N'_x\tilde{N}_x), \quad (2.7)$$

$$\{H_{\text{gr}}(N), H_x(N_x)\} = H_{\text{gr}}(N_x N'), \quad (2.8)$$

$$\{H_{\text{gr}}(N), H_{\text{gr}}(\tilde{N})\} = H_x \left(\frac{|E^x|}{(E^\varphi)^2} [N\tilde{N}' - N'\tilde{N}] \right), \quad (2.9)$$

as usual, involves structure functions. To Abelianize the algebra of the Hamiltonian constraint with itself, we follow the ideas of [7–9] and introduce new lapse and shift functions as follows

$$N^x = \bar{N}^x - 2N \frac{K_\varphi \sqrt{|E^x|}}{(E^x)'}, \quad N = \bar{N} \frac{(E^x)'}{E^\varphi}, \quad (2.10)$$

which changes the scalar constraint while leaving the diffeomorphism constraint unchanged

$$\bar{H}(\bar{N}) = - \int dx \bar{N} \left[\left(\sqrt{|E^x|} \left(1 + K_\varphi^2 - \frac{[(E^x)']^2}{4(E^\varphi)^2} \right) \right)' - \sqrt{|E^x|} (E^x)' \frac{\Lambda}{2} \right], \quad (2.11)$$

$$H_x(\bar{N}^x) = \int dx \bar{N}^x [-(E^x)' K_x + E^\varphi K_\varphi']. \quad (2.12)$$

Rewriting $\sqrt{|E^x|} (E^x)' \Lambda/2$ as $[|E^x|^{3/2} \Lambda/3]'$ and then integrating by parts we obtain

$$H_{\text{ab}}(\tilde{N}) = - \int dx \tilde{N} \left[-\sqrt{|E^x|} \left(1 + K_\varphi^2 - \frac{[(E^x)']^2}{4(E^\varphi)^2} \right) + 2GM + |E^x|^{3/2} \frac{\Lambda}{3} \right] \quad (2.13)$$

where $\tilde{N} := \bar{N}'$ is the new lapse function. The term $2GM$ can be introduced either by imposing appropriate boundary conditions to ensure the existence of Schwarzschild-like solutions [7, 8, 10] in the limit of vanishing cosmological constant, or by noticing that it is actually a Dirac observable as shown in [10, 12]. The Hamiltonian constraint now has an Abelian algebra with itself and the usual algebra with the diffeomorphism constraint,

$$\{H_{\text{ab}}(\tilde{N}), H_{\text{ab}}(\tilde{M})\} = 0, \quad (2.14)$$

$$\{H(\tilde{N}), H_x(\tilde{N}_x)\} = H_{\text{ab}}(\tilde{N}_x \tilde{N}'), \quad (2.15)$$

$$\{H_x(\tilde{N}_x), H_x(\tilde{M}_x)\} = H_x(\tilde{N}_x \tilde{M}'_x - \tilde{N}'_x \tilde{M}_x). \quad (2.16)$$

Classically, as it was shown in [7] for the Schwarzschild spacetime, the Hamiltonian constraint (2.13) can be factorized as $H_{\text{ab}}(\tilde{N}) = \int dx \tilde{N} H_- H_+$ where

$$H_\pm = \sqrt{\sqrt{|E^x|} (1 + K_\varphi^2) - 2GM - |E^x|^{3/2} \frac{\Lambda}{3}} \pm \frac{(E^x)' |E^x|^{1/4}}{2E^\varphi}. \quad (2.17)$$

Classically E^x , $(E^x)'$ and E^φ are positive definite, hence the vanishing of the Hamiltonian constraint can then be taken to correspond to $H_- = 0$. This simplification leads to a first order differential equation in the quantum theory for the physical states (see Appendix A). Accordingly, we redefine the lapse to be $\underline{N} = \tilde{N} H_+ / 2E^\varphi$ to rewrite the Hamiltonian constraint in the form

$$H_{\text{ab}}(\underline{N}) = \int dx \underline{N} \left(2E^\varphi \sqrt{\sqrt{|E^x|} (1 + K_\varphi^2) - 2GM - |E^x|^{3/2} \frac{\Lambda}{3}} - (E^x)' |E^x|^{1/4} \right). \quad (2.18)$$

Classically, the constraints can be easily solved. For simplicity, we restrict to the stationary slicing which corresponds to $\bar{N}^x = 0$ and $\tilde{N} = 0$, yielding $N = a(E^x)' / E_\varphi$ and $N^x = -2NK_\varphi \sqrt{|E^x|} / (E^x)'$, where a is a constant of integration. The two constraints reduce two degrees of freedom per spacetime point, leaving two residual gauge degrees of freedom. To fully gauge-fix the theory, we use two functional parameters to express two of the phase space variables as

$$E^x = g(x), \quad K_\varphi = h(x). \quad (2.19)$$

With these choices, the theory can be consistently solved to yield the remaining phase space variables as

$$(E^\varphi(x))^2 = \frac{g'(x)^2/4}{1 + h^2(x) - \frac{2GM}{\sqrt{g(x)}} - \frac{\Lambda}{3}g(x)}, \quad (2.20)$$

$$K_x(x) = \frac{h'(x)/2}{\sqrt{1 + h^2(x) - \frac{2GM}{\sqrt{g(x)}} - \frac{\Lambda}{3}g(x)}}, \quad (2.21)$$

where we require that $g(x) > 0$ and $g'(x) \neq 0$. Different choices of the arbitrary functions $h(x)$ and $g(x)$ correspond to different coordinate choices for the stationary spacetimes represented by our theory. In order to fix the constant of integration in the lapse function, we further require that the resulting spacetimes in the limit of vanishing cosmological constant to be asymptotically flat [7, 8, 10]. We then must have $g(x) = x^2 + O(x^{-1})$ and $h(x) = O(x^{-1})$ when $x \rightarrow \infty$. This determines the integration constant in N to be $a = 1/2$. Thus we finally have

$$N^2 = 1 + h^2(x) - \frac{2GM}{\sqrt{g(x)}} - \frac{\Lambda}{3}g(x), \quad (2.22)$$

$$N^x = -\frac{2h(x)\sqrt{g(x)}}{g'(x)} \sqrt{1 + h^2(x) - \frac{2GM}{\sqrt{g(x)}} - \frac{\Lambda}{3}g(x)}. \quad (2.23)$$

III. QUANTUM THEORY: KINEMATICS OF THE IMPROVED DYNAMICS SCHEME

The kinematical Hilbert space of loop quantum gravity is the space of cylindrical functions of the holonomies of the connections defined over arbitrary graphs, where the spin network states provide an orthonormal basis for this space [21–23]. For our reduced spherically symmetric model, the details of these spin network states and the kinematical Hilbert space are extensively discussed in previous works [7–9, 11, 13]. The basic elements are one-dimensional oriented graphs g with support in the radial direction, which are composed by edges $\{e_j\}$ along the radial direction connecting the vertices $\{v_j\}$. The connection component K_x is associated with holonomies in the radial direction and K_φ with point holonomies on the vertices. We follow the construction suggested in [14, 16] and consider spin networks with a finite but arbitrarily large number of edges and vertices. The kinematical Hilbert space of the reduced model has a basis of spin network states $|\vec{k}, \vec{\mu}\rangle$, with $k_j \in \mathbb{Z}$ the valences of the edges e_j and $\mu_j \in \mathbb{R}$ and the valences of the vertices v_j . The action of the triad operators on this basis is given by

$$\hat{E}^x(x_j)|\vec{k}, \vec{\mu}\rangle = \ell_{Pl}^2 k_j |\vec{k}, \vec{\mu}\rangle \quad \text{if } x_j \in e_j, \quad (3.1)$$

$$\hat{E}^\varphi(x)|\vec{k}, \vec{\mu}\rangle = \sum_{v_j} \delta(x - x_j) \ell_{Pl}^2 \mu_j |\vec{k}, \vec{\mu}\rangle, \quad (3.2)$$

It is worth commenting that $(\ell_{Pl}^2 k_j)$, the eigenvalues of $\hat{E}^x(x)$, can be naturally identified with areas of the sphere of symmetry normalized by the unit sphere area. However, the eigenvalues of $\hat{E}^\varphi(x)$ have no invariant geometrical meaning since the classical analog is a scalar density (is not invariant under coordinate transformations).

The variables conjugate to the triads in the quantum theory are the holonomies of the connections along the edges of the graph. The Abelianized Hamiltonian constraint (2.13) only contains the connection component K_φ , which is represented in the quantum theory by point holonomies $\hat{U}_{\rho_j} := \exp(i\rho_j \widehat{K_\varphi}(x_j))$ which act on the vertices. Their action on the basis states is given as

$$\hat{U}_{\rho_j}(x_j)|\vec{k}, \vec{\mu}\rangle = |\vec{k}, \vec{\mu}'\rangle, \quad (3.3)$$

where $\vec{\mu}'$ is obtained from $\vec{\mu}$ by modifying the valence μ_j of the vertex located at x_j by $\mu_j + \rho_j$.

Before we proceed with the quantization program, it is worth introducing here the improved dynamics scheme following the ideas in [18] and [16, 17, 19]. It allows us to fix various deformation parameters that appear in the theory, while they respect the simplicity of the above kinematics which will still be suitable for further calculations. The motivation is that, classically, the curvature components at a point are equivalent to the holonomies of the connection around infinitesimal

closed loops along suitable directions. However in LQG, various geometric operators such as area and volume have discrete spectra. Thus, the curvature components in LQG are approximated by holonomies around plaquettes which enclose the smallest (finite) possible area allowed by the theory, which in this case we choose to equal the minimum eigenvalue of the area operator in LQG, denoted by Δ . In this reduced model we choose the plaquettes to be well adapted to the Killing symmetries which, once equated to the minimum area eigenvalue, yielding relations which fix the kinematical parameters.

Concretely, let us first consider the plaquettes adapted to the 2-spheres at each vertex. Classically the 2-spheres have a physical area given by $4\pi g_{\theta\theta}(x) = 4\pi E^x(x)$. In order to impose the improved dynamics prescription, we assume that the areas of the 2-spheres in the effective geometry obtained from the quantum dynamics are well approximated by replacing E^x in the above expression by its eigenvalue given in (3.1). The validity of this assumption rests on whether we obtain a self-consistent and physically sensible quantization at the end of the day. The plaquette on the $\theta - \phi$ sector will hence enclose an area given by $4\pi\ell_{Pl}^2|k_j|\rho_j^2$ which must be equal to the minimum area eigenvalue, Δ , which yields

$$\rho_j = \sqrt{\frac{\Delta}{4\pi\ell_{Pl}^2|k_j|}}. \quad (3.4)$$

This suggests a more convenient state relabeling as $|\nu_j\rangle$ where $\nu_j = \mu_j\sqrt{4\pi\ell_{Pl}^2|k_j|/\Delta}$. This simplifies the action of the point holonomies as

$$\hat{U}_{\rho_j}|\nu_j\rangle = |\nu_j + 1\rangle. \quad (3.5)$$

The physical meaning of this label was discussed in [17] and can be naturally identified to be proportional to the local volume operator $\hat{V}(x_j) = \sqrt{|\hat{E}^x(x_j)|\hat{E}^\varphi(x_j)}$.

Further, as introduced in [16], we implement a second improved dynamics condition on the plaquettes in the $\theta - x$ and $\varphi - x$ planes, which lead to only one additional condition due to spherical symmetry. We set these plaquettes in the equatorial plane ($\theta = \pi/2$) without loss of generality. Classically, infinitesimal lengths along the x and φ directions are equal to the norms of the 1-forms $(dx)^\mu$ and $(d\varphi)^\mu$ respectively. Thus the area of an infinitesimal plaquette in the equatorial plane can be written as $(\sqrt{|g_{\mu\nu}|}(dx)^\mu(dx)^\nu\sqrt{|g_{\mu\nu}|}(d\varphi)^\mu(d\varphi)^\nu)$. This expression for the area is coordinate independent, so we can simplify it by going to the diagonal gauge in which the metric is diagonal (this amounts to setting $h(x) = 0$), leading to the expression $(\sqrt{|g_{xx}|}dx\sqrt{|g_{\theta\theta}|}d\varphi)$ for the area in the diagonal gauge. This leads to the improved dynamics condition

$$2\pi\sqrt{|g_{xx}(x_j)|}\delta x_j\sqrt{|g_{\theta\theta}(x_j)|}\rho_j = \Delta, \quad (3.6)$$

at the vertex v_j , where $2\pi\rho_j$ is the coordinate length along the φ - direction and δx_j is the coordinate length along the x - direction, namely, of the edge e_j of the spin network as per our kinematical scheme described above. For simplicity, we will not impose this condition at all vertices, but only in the vertex where we expect quantum corrections will be largest. This suggests a choice of spin networks that show an equal spacing in a suitable radial coordinate, such that $\delta x_j = \delta x$. In particular, we will restrict our analysis, without loss of generality, to spin networks such that

$$\hat{E}^x(x)|\vec{k}, \vec{v}\rangle = \ell_{Pl}^2 k_j |\vec{k}, \vec{v}\rangle = \text{sign}(x_j)(x_j^2 + x_0^2)|\vec{k}, \vec{v}\rangle, \quad (3.7)$$

where

$$x_j = j\delta x \quad \text{if } j \in [-S, -1], \quad (3.8)$$

$$x_j = (j - 1)\delta x \quad \text{if } j \in [1, S], \quad (3.9)$$

such that $(\delta x/\ell_{Pl}) \in \mathbb{N}$. This construction follows from [14, 16].

The required classical metric components in the diagonal gauge for the above improved dynamics conditions are given by

$$g_{\theta\theta}(x) = E^x(x), \quad g_{xx}(x) = \frac{(E^\varphi(x))^2}{|E^x(x)|} = \frac{([E^x(x)]')^2}{4E^x(x)} \frac{1}{1 - \frac{2GM}{\sqrt{E^x(x)}} - \frac{\Lambda}{3}E^x(x)}, \quad (3.10)$$

where we have used equation (2.20) in the last expression. Following [16], we approximate $([E^x(x)]')^2$ by $(2\sqrt{x_j^2 + \Delta^2/x_0^2} + \delta x)^2$, which agrees with the exact expression up to corrections of the order Δ^2/x_0^2 , which will be negligible for macroscopic black holes, as we will see. With these choices, the improved dynamics condition (3.6) evaluated at $j = 1$, reduces to

$$\frac{(2\Delta/x_0 + \delta x)}{\sqrt{1 - \frac{2GM}{x_0} - \frac{\Lambda x_0^2}{3}}} = \sqrt{\frac{\Delta}{\pi}}, \quad (3.11)$$

where we have used the first improved dynamics condition (3.4) to substitute for ρ_j .

IV. PHYSICAL STATES AND OBSERVABLES

The quantum dynamics of the model is summarized in Appendix A. On physical states, the kinematical operators like (\hat{E}^x) and $(\hat{E}^\varphi)^2$ are written as parameterized observables. This implies they can be expressed in terms of both Dirac observables and functional parameters, the latter possibly being also functions of Dirac observables. Concretely,

$$\hat{E}^x(x) = \hat{O}_{z(x)}, \quad \widehat{[E^x(x)]'} = \frac{\hat{O}_{z(x)+1/S} - \hat{O}_{z(x)}}{x(z+1/S) - x(z)}, \quad (4.1)$$

$$(\hat{E}^\varphi(x_j))^2 = \frac{([\hat{E}^x(x_j)]')^2/4}{1 + \frac{\sin^2(\rho_j K_\varphi(x_j))}{\rho_j^2} - \frac{2GM}{\sqrt{|\hat{E}^x(x_j)|}} - \frac{\Lambda}{3}|\hat{E}^x(x_j)|}, \quad (4.2)$$

where $2S$ is the total number of vertices. In order for $(\hat{E}^\varphi)^2$ to be a well-defined self-adjoint operator, it must satisfy $(\hat{E}^\varphi(x_j))^2 > 0$. From the above expression, we see that there are two ways that $(\hat{E}^\varphi(x_j))^2$ may fail to be positive-definite - either when the cosmological constant is positive and the product $\Lambda|\hat{E}^x|$ becomes too large, or when $|\hat{E}^x|$ is too small. We will see that this leads to an upper bound for Λ and a lower bound for $|\hat{E}^x|$ in order for $(\hat{E}^\varphi(x_j))^2$ to be well-defined. To understand this, we identify the source of the problem in different regimes.

Let us first focus on the asymptotic region where $|\hat{E}^x|$ is macroscopic and large, i.e. $|\hat{E}^x| \approx x_j^2$ where j is so large that we may approximate it by a continuous label. In this regime, the improved dynamics condition (3.4) implies that ρ_j is vanishingly small. For choices of the gauge function $K_\varphi(x_j)$ such that $\sin^2(\rho_j K_\varphi(x_j)) \simeq \rho_j^2 K_\varphi^2(x_j) \simeq \mathcal{O}(x_j^{-\alpha})$ with $\alpha \geq 0$, the quantum expression (4.2) for $(\hat{E}^\varphi(x_j))^2$ reduces to the classical expression (2.20), as expected. However, when Λ is positive, the classical expression (2.20) for $[E^\varphi(x_j)]^2$ itself may be ill-defined when $E^x(x)$ exceeds a certain maximum value (say at $E^x(x) = x_L$), which depends on Λ , M and the choice of gauge function $h(x)$ provided it is chosen such that it does not grow as x^2). If x_L is large enough, one may be inclined to think that we are far from the strongly quantum region at the centre, and classical expressions should faithfully approximate quantum dynamics in any valid gauge choice. Consequently, we may conclude that we need not view the failure of $[E^\varphi(x_j)]^2$ to be positive-definite as a problem with the quantization, or putting a limit on how large a positive Λ can be, as we are already at the

classical level where this can be easily addressed by making a different gauge choice for $h(x)$ where the slicing will be valid beyond x_L , as shown for example in the next section with Eddington-Finkelstein coordinates where this problem disappears. However, as we find out in section VB that it turns out to be more than a mere failure of the choice of slicing. In particular, we find that the curvature of spacetime in the asymptotic limit is of the order of Λ . The curvature in the asymptotic limit may be arbitrarily large if Λ is allowed to be arbitrarily large. However, we expect quantum effects to kick in when the curvature is positive and approaches Planckian values. Thus, quantum effects must be significant in the asymptotic region when $\Lambda > 0$ and approaches Planckian values. This is not manifest in Eddington-Finkelstein coordinates used in the next section until one computes the curvature in the asymptotic region. Fortunately, our choice of gauge here makes the problem manifest by making $(\hat{E}^\varphi)^2$ ill-defined when $\Lambda > 0$ and exceeds a certain Planckian bound. This can be seen as follows. In order for $(\hat{E}^\varphi)^2$ to be well-defined, the denominator in equation (4.2) must be positive-definite. The best we can do at the quantum level is to choose $\rho_j K_\varphi(x_j) = \pi/2$, implying that the two positive terms in the denominator of (4.2) have a global maximum given by $1 + 1/\rho_j^2$, independent of the choice of gauge (but is manifest for the choice made few line above). This leads to the condition

$$1 + \frac{4\pi(x_j^2 + x_0^2)}{\Delta} - \frac{2GM}{\sqrt{x_j^2 + x_0^2}} - \frac{\Lambda}{3}(x_j^2 + x_0^2) > 0, \quad \forall \quad x_j, M, \Lambda \quad (4.3)$$

where we have substituted for ρ_j from (3.4). In order to obtain nontrivial semiclassical spacetimes, the choice of Λ must allow for an arbitrary number of vertices such that we can take the limit $\ell_{Pl}^2 k_j = x_j^2 \rightarrow +\infty$. In the asymptotic limit $x_j \rightarrow \infty$, the above condition leads to a mass-independent Planckian upper bound on the cosmological constant given by

$$\Lambda < \Lambda_{max} = \frac{12\pi}{\Delta}. \quad (4.4)$$

In other words, the cosmological constant must satisfy $-\infty < \Lambda < \Lambda_{max}$. It is an interesting question whether a quantization of the Schwarzschild-deSitter spacetime consistent with Λ greater than this threshold can be obtained. In the case of homogeneous deSitter cosmologies [24, 25], it was possible to study the spectrum of the Hamiltonian constraint operator, and it was not possible to find normalizable physical states for a positive Λ larger than a critical (Planck order) value. Hence, the quantum theory provided a nontrivial bound $\rho_\Lambda < \rho_c = 3/\Delta$. Here, we find a similar result but for spherically symmetric spacetimes. As we shall see in the next section, the curvature invariants in the asymptotic limit are proportional to Λ . Thus, this Planckian upper bound on Λ coming from the quantization serves to ensure that the curvature cannot exceed a certain positive Planckian upper bound in the asymptotic limit.

Note that our quantization does not lead to an upper bound on the magnitude of Λ when it is negative. In other words, for the Schwarzschild-anti-deSitter spacetimes for which the curvature in the asymptotic limit is again proportional to Λ and hence negative, our quantization in principle allows to choose a negative Λ larger than Planckian values which makes the negative curvature at conformal infinity larger than Planckian. While this is of little phenomenological interest as the observed values of Λ are insignificantly small, but it is conceptually significant. Note that unlike the deSitter cosmology, loop quantization of the homogeneous anti-de Sitter spacetime also does not lead to any upper bound on the negative Λ [26]. These results seem to suggest that quantum gravity does not treat a finite negative curvature (a repulsive gravitational field), however large, as a problem. Intuitively, a repulsive gravitational field does not lead to the kind of runaway catastrophic phenomenon (such as gravitational collapse) that an attractive field does if it is too large. Therefore, no limit is obtained on how large a negative Λ can be.

We must also look at the consequences of the condition (4.3) in the regime where $x_j \rightarrow 0$. This is the quantum regime when the holonomies are nearly saturated and $\hat{E}^x = x_0^2$ (corresponding to the minimum area 2-spheres). This leads to the condition

$$1 + \left(\frac{4\pi}{\Delta} - \frac{\Lambda}{3} \right) x_0^2 - \frac{2GM}{x_0} > 0 \quad \forall \quad M, \Lambda. \quad (4.5)$$

Given M and $-\infty < \Lambda < \Lambda_{max}$, this leads to a lower bound on x_0 , which can be found as follows. We look at the roots of the following expression

$$\sigma = 1 + \left(\frac{4\pi}{\Delta} - \frac{\Lambda}{3} \right) x_0^2 - \frac{2GM}{x_0} \quad (4.6)$$

which are the same as the roots of the polynomial $x_0 - 2GM + Ax_0^3$ where $A = (4\pi/\Delta - \Lambda/3)$. Since $\Lambda < 12\pi/\Delta$ as per the condition (4.4), A is positive definite and the discriminant of the above cubic polynomial is negative definite, implying the existence of a single real root, which provides a lower bound for x_0 below which the expression σ is negative and the condition (4.6) is violated. In the limit $2GM \gg \ell_{Pl}$ and $|\Lambda| \ll 12\pi/\Delta$, the lower bound on x_0 is given by

$$x_0^{min} \approx \left(\frac{2GM}{4\pi/\Delta - \Lambda/3} \right)^{1/3}. \quad (4.7)$$

Thus the condition (4.3) has led us to the conclusion that we must only consider spin networks which have support on eigenvalues of the operator $\hat{E}^x(x)$ greater than $(x_0^{min})^2$. Moreover, in the limit $|\Lambda| \ll 12\pi/\Delta$, $2GM \gg \ell_{Pl}$, the second improved dynamics condition implies

$$\delta x \approx 2\ell_{Pl} \text{Int} \left[\frac{x_0^{min}}{\ell_{Pl}} \right], \quad (4.8)$$

at leading order. Thus we see that the two improved dynamics conditions (3.4) and (3.11) and the condition (4.3) help us fix three of the kinematical parameters x_0 , ρ_0 and δx , which in turn fix the rest of the kinematical parameters.

As shown in [16], the leading order term in the value obtained for x_0^{min} , which is $(2GM\Delta/4\pi)^{1/3}$ is the same as that for the charged black hole analyzed in [16] as well as the uncharged Schwarzschild black hole studied in [19, 20] in the improved dynamics scheme. The small corrections to the leading order term produced at the first order by the presence of a tiny cosmological constant in this manuscript are positive in contrast to the charged black hole considered in [16], where the first order corrections due to presence of a tiny amount of charge are negative.¹

V. EFFECTIVE GEOMETRY

In this section, we obtain the effective metric from the above quantization in the improved dynamics, which will help us study its physical aspects. The effective metric is also crucial in analyzing various phenomenological properties of the quantized spacetime. In order to compare with previous quantizations of the Schwarzschild black hole [19, 20] and the charged black hole [16]

¹ For a solar mass black hole, $x_0^{min} \simeq 10^{-23}m \simeq 10^{12}\ell_{Pl}$ at the leading order. For supermassive black holes with masses about a billion times that of the sun $x_0^{min} \simeq 10^{-20}m$. Thus x_0^{min} would be microscopic even for the largest known black holes.

using improved dynamics, we use the same slicing in this section as used in these studies, which leads to Eddington-Finkelstein coordinates. As we will see, this will also alleviate the difficulties in analyzing the asymptotic region in the presence of the cosmological constant as commented in the previous section. The Eddington-Finkelstein horizon penetrating coordinates amount to the following gauge fixing [19, 20]

$$\frac{\sin^2(\widehat{\rho_j K_\varphi}(x_j))}{\rho_j^2} = \frac{\left(\frac{2G\hat{M}}{\sqrt{|\hat{E}^x(x_j)|}} + \frac{\Lambda}{3}|\hat{E}^x(x_j)|\right)^2}{1 + \frac{2G\hat{M}}{\sqrt{|\hat{E}^x(x_j)|}} + \frac{\Lambda}{3}|\hat{E}^x(x_j)|}. \quad (5.1)$$

Equations (2.22) and (2.23) immediately let us obtain the operator expressions for lapse and shift in this case. using equation (2.20), we find that

$$(\hat{E}^\varphi(x_j))^2 = \frac{([\hat{E}^x(x_j)]')^2}{4} \left(1 + \frac{2G\hat{M}}{\sqrt{|\hat{E}^x(x_j)|}} + \frac{\Lambda}{3}|\hat{E}^x(x_j)|\right), \quad (5.2)$$

which is positive definite in the Eddington-Finkelstein coordinates. Treating the metric components given in (2.6) as parameterized observables, their operators are given by

$$\hat{g}_{xx}(x_j) = \frac{(\hat{E}^\varphi(x_j))^2}{|\hat{E}^x(x_j)|} = \frac{([\hat{E}^x(x_j)]')^2}{4|\hat{E}^x(x_j)|} \left(1 + \frac{2G\hat{M}}{\sqrt{|\hat{E}^x(x_j)|}} + \frac{\Lambda}{3}|\hat{E}^x(x_j)|\right), \quad (5.3)$$

$$\hat{g}_{tx}(x_j) = \hat{g}_{xt}(x_j) = N_x = g_{xx}N^x = -\frac{[\hat{E}^x(x_j)]'}{2\sqrt{|\hat{E}^x(x_j)|}} \left(\frac{2G\hat{M}}{\sqrt{|\hat{E}^x(x_j)|}} + \frac{\Lambda}{3}|\hat{E}^x(x_j)|\right), \quad (5.4)$$

$$\hat{g}_{tt}(x_j) = -(N^2 - N_x N^x) = -\left(1 - \frac{2G\hat{M}}{\sqrt{|\hat{E}^x(x_j)|}} - \frac{\Lambda}{3}|\hat{E}^x(x_j)|\right), \quad (5.5)$$

$$\hat{g}_{\theta\theta}(x_j) = |\hat{E}^x(x_j)|, \quad \hat{g}_{\varphi\varphi}(x_j) = |\hat{E}^x(x_j)| \sin^2 \theta. \quad (5.6)$$

To obtain the effective metric, we follow the strategy used in [19]. We restrict to a single spin network and consider a family of states sharply peaked in both M and Λ at values which are consistent with the requirement (4.7). The details of the construction are analogous to that of [19]. An effective spacetime can then be defined as the one obtained by computing the expectation values of the metric operators on these sharply peaked states, i.e. $g_{\mu\nu} = \langle \hat{g}_{\mu\nu} \rangle$. While we have already neglected the effects emerging from superpositions of several spin network states, this effective metric still inherits several quantum corrections from the underlying quantum theory, namely (i) the lower bound (4.7) on the value of $\hat{E}^x(x)$, (ii) corrections due to polymerization of the curvature components, (iii) the inherent discreteness in derivatives such as $[\hat{E}^x(x_j)]'$ and the derivatives of the metric needed to compute curvature components, and (iv) superpositions in the \hat{M} and $\hat{\Lambda}$. However, here we focus only on the most prominent effects which are due to (i) and (ii). We ignore the subleading contributions due to the spread ΔM and $\Delta \Lambda$ in mass and cosmological constant. These effects are discussed in [19]. And for simplicity, we ignore the effects of discreteness of the spectrum of $\hat{E}^x(x)$ and the discreteness of all the derivative terms, emerging from the fact that we have a finite number of discrete vertices. We assume we are working at a certain coarse-grained level where we can replace x_j with a continuous variable x . The justification for this simplification is also provided in [19], where numerical values of the discrete and coarse-grained expressions of the second derivatives of the metric are compared to show the error incurred in coarse-graining

is at most 10% in the most quantum region, which quickly becomes negligible as we move to low curvature regions. Under these assumptions, the effective metric can be written as $g_{\mu\nu} = {}^{(0)}\hat{g}_{\mu\nu} + \dots$, where ${}^{(0)}\hat{g}_{\mu\nu}$ contains only the corrections due to effects (i) and (ii) and is given by

$$\begin{aligned} {}^{(0)}ds^2 : = {}^{(0)}\hat{g}_{\mu\nu}dx^\mu dx^\nu = & -f(x)dt^2 - 2(1-f(x))\frac{\left(\sqrt{x^2 + \Delta^2/(x_0^{min})^2} + x_0^{min}\right)}{\sqrt{x^2 + (x_0^{min})^2}}dtdx \\ & + (2-f(x))\frac{\left(\sqrt{x^2 + \Delta^2/(x_0^{min})^2} + x_0^{min}\right)^2}{x^2 + (x_0^{min})^2}dx^2 + (x^2 + (x_0^{min})^2)d\Omega^2, \end{aligned} \quad (5.7)$$

where

$$f(x) = 1 - \frac{2GM}{\sqrt{x^2 + (x_0^{min})^2}} - \frac{\Lambda}{3}(x^2 + (x_0^{min})^2), \quad (5.8)$$

where we have used (4.8) to replace δx .

A. Causal structure of the effective spacetime

As we investigate the causal structure, we find that there are four distinct spacetimes depending on the value of the cosmological constant. We describe the causal structure of the effective spacetime for all four possibilities.

Firstly, to locate if there are any horizons, we consider the timelike Killing vector field $t^\mu = (1, 0, 0, 0)$. Its norm is given by $t^\mu t_\mu = -f(x)$, indicating that the roots of the equation $f(x) = 0$ correspond to surfaces $x = \text{contant}$ on which the timelike Killing vector field becomes null. Thus, the location of horizons is given by

$$1 - \frac{2GM}{\sqrt{x^2 + (x_0^{min})^2}} - \frac{\Lambda}{3}(x^2 + (x_0^{min})^2) = 0. \quad (5.9)$$

However, if we make the substitution

$$r^2 = x^2 + (x_0^{min})^2, \quad x > 0, \quad r > 0, \quad (5.10)$$

then the above condition reduces to the corresponding condition for the classical SdS spacetime given by

$$1 - \frac{2GM}{r} - \frac{\Lambda}{3}r^2 = 0, \quad (5.11)$$

whose roots are well known. In the above expression, we have kept the positive square root of $(x^2 + (x_0^{min})^2)$ only. The nature of the roots of the equation (5.11) depends on the value of Λ . We now describe all the possibilities one by one.

1. Schwarzschild deSitter spacetime with $0 < 9G^2M^2\Lambda < 1$

When $0 < \Lambda < 1/9G^2M^2$ (small spacetime masses), Eq. (5.11) has three real roots, two of which are positive (and physical since we choose $r > 0$) given by

$$r_{\pm} = -\frac{2}{\sqrt{\Lambda}} \cos\left(\frac{1}{3} \cos^{-1}(3GM\sqrt{\Lambda}) \pm \frac{2\pi}{3}\right). \quad (5.12)$$

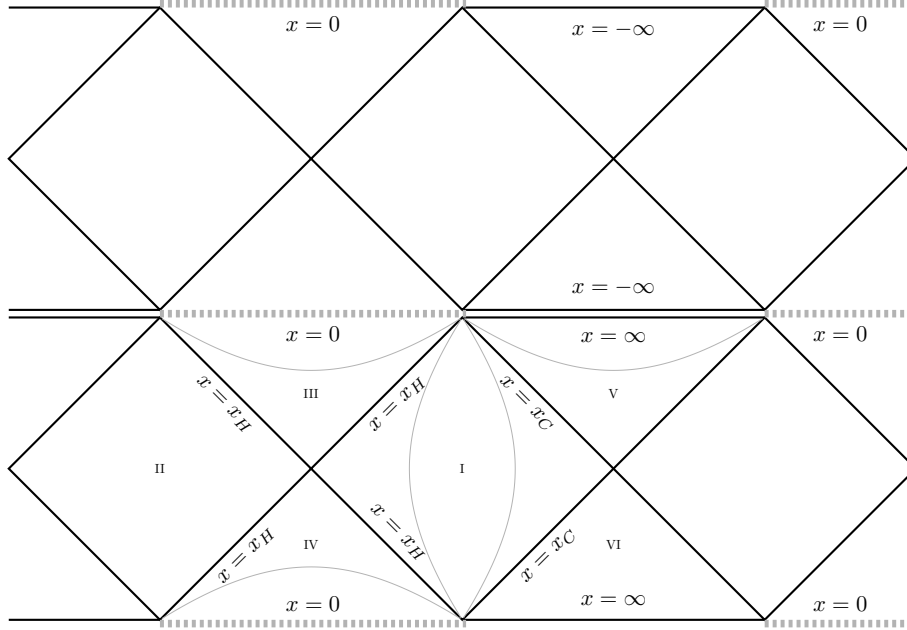


FIG. 1: Penrose diagram for $\Lambda < 1/9G^2M^2$.

Here $r_+ > r_- > 0$. Classically, there is a cosmological horizon at r_+ and a black hole horizon at r_- . Using these and equation (5.10), we can easily obtain the horizons for the effective geometry as follows

$$x_{\pm} = \sqrt{r_{\pm}^2 - (x_0^{min})^2}. \quad (5.13)$$

These two positive roots $\sqrt{r_{\pm}^2 - (x_0^{min})^2}$ correspond to the cosmological and black hole horizons just as in the classical SdS spacetime. Note that the effective geometry is regular at $x = 0$ and the spacetime can be extended to negative values of x . Thus we also have the roots corresponding to negative values of x . If we define $\tilde{r}^2 = x^2 + (x_0^{min})^2$ for $x < 0$ and with $\tilde{r} > 0$, and inserting it in Eq. (5.11), we obtain three real roots, two of them being positive (and physical), given by $\tilde{x}_{\pm} = -\sqrt{r_{\pm}^2 - (x_0^{min})^2}$. They correspond to the white hole horizon after the anti-trapped region in the effective spacetime (\tilde{x}_-) and the corresponding cosmological horizon (\tilde{x}_+).

In Figure 1, we show the Penrose diagram for this configuration where $0 < \Lambda < 1/9G^2M^2$. The main difference with the classical spacetime is that the singularity at $x = 0$ is replaced by a transition surface connecting a trapped region (black hole interior) with an antitrapped region (white hole interior). Therefore, an observer falling into a black hole region will eventually pop up into another universe (after crossing the corresponding white hole horizon), and can either remain in the exterior region, fall into the corresponding black hole, or cross the cosmological horizon and reach the asymptotic infinity which now is a spacelike surface.

2. Schwarzschild deSitter spacetime with $9G^2M^2\Lambda > 1$

In the case of ultramassive spacetimes, namely, when $\Lambda > 1/9G^2M^2$, the Killing vector field t^{μ} is always spacelike, while ∂_x is always timelike and past directed. Hence, these spacetimes are homogeneous but anisotropic. In other words, the whole spacetime is free of horizons. It is conformed by a trapped region for $x > 0$ and an anti-trapped region for $x < 0$. Since the radial

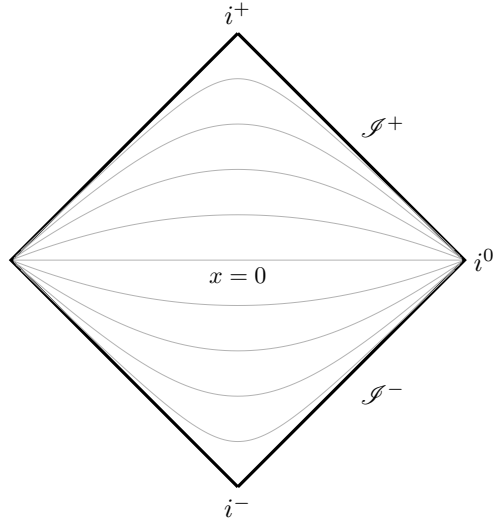


FIG. 2: Penrose diagram for $\Lambda > 1/9G^2M^2$.

coordinate becomes timelike and vice-versa, let us refer to the corresponding coordinates as $(\mathcal{T}, \mathcal{X})$. The line element, in the diagonal gauge, takes the form:

$${}^{(0)}ds^2 : = -\frac{1}{f(\mathcal{T})} \frac{\left(\sqrt{\mathcal{T}^2 + \Delta^2/\mathcal{T}_0^2} + \mathcal{T}_0\right)^2}{\mathcal{T}^2 + \mathcal{T}_0^2} d\mathcal{T}^2 + f(\mathcal{T}) d\mathcal{X}^2 + (\mathcal{T}^2 + \mathcal{T}_0^2) d\Omega^2, \quad (5.14)$$

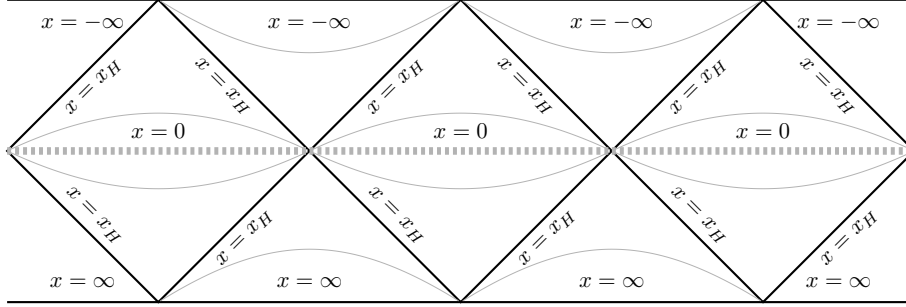
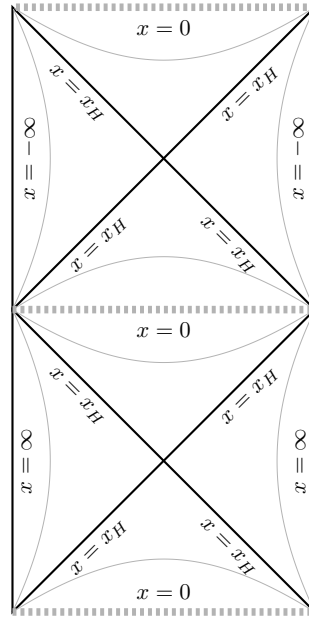
with

$$f(\mathcal{T}) = \frac{\Lambda}{3} (\mathcal{T}^2 + \mathcal{T}_0^2) + \frac{2GM}{\sqrt{\mathcal{T}_0^2 + \mathcal{T}_0^2}} - 1. \quad (5.15)$$

In Figure 2, we show the corresponding Penrose diagram. The region $x > 0$ (i.e. $\mathcal{T} > 0$) corresponds to a trapped (collapsing) spacetime that reaches a Plankian curvature at $x = 0$ (i.e. $\mathcal{T} = 0$) and eventually transitions into an antitrapped (expanding) region $x < 0$ (i.e. $\mathcal{T} < 0$). Hence, this scenario can be understood as a bouncing (anisotropic) cosmological model. We must keep in mind that the cosmological constant must still be bounded by Eq. (4.4).

3. Schwarzschild deSitter spacetime with $9G^2M^2\Lambda = 1$

Let us now discuss the particular case $\Lambda = 1/9G^2M^2$. Here, the two horizons given by (5.11) coincide when $\Lambda = 1/9G^2M^2$ and the spacetime only has one horizon. The coordinate x is null at the horizon and spacelike everywhere else while t is temporal. The causal structure in this case is depicted in the Penrose diagram in Figure 3. In this case observers emanate from the spatial infinity and cross the black hole horizon, entering a trapped region. Since the singularity at $x = 0$ is resolved, the observers cross it entering an anti-trapped region and eventually come out of the white hole horizon, finally approaching the corresponding spatial infinity again.

FIG. 3: Penrose diagram for the extremal case $\Lambda = 1/9G^2M^2$.FIG. 4: Penrose diagram for $\Lambda < 0$.

4. Schwarzschild Anti-deSitter spacetime with $\Lambda < 0$

Finally, when $\Lambda < 0$, the equation (5.11) has a single positive root given by

$$r_h = \left(\frac{3GM}{\Lambda}\right)^{1/3} \left[(C+1)^{1/3} - (C-1)^{1/3} \right], \quad \text{where } C = \sqrt{1 - \frac{1}{9G^2M^2\Lambda}}. \quad (5.16)$$

This single root r_h corresponds to the black/white hole horizon. There is no cosmological horizon in this case. The causal structure in this case is depicted in Fig. 4. The spacetime is asymptotically anti-deSitter and the conformal infinity $x = \infty$ is timelike.

B. Curvature of the effective spacetime

We now use the effective metric (5.7) to analyze the properties of the curvature invariants of the effective spacetime such as the Ricci scalar $R = R_{\mu\nu}g^{\mu\nu}$, the Kretschmann scalar $K = R_{\mu\nu\rho\lambda}R^{\mu\nu\rho\lambda}$ and the Ricci tensor squared $R_{\mu\nu}R^{\mu\nu}$. In the most quantum region around $x = 0$ and in the limit

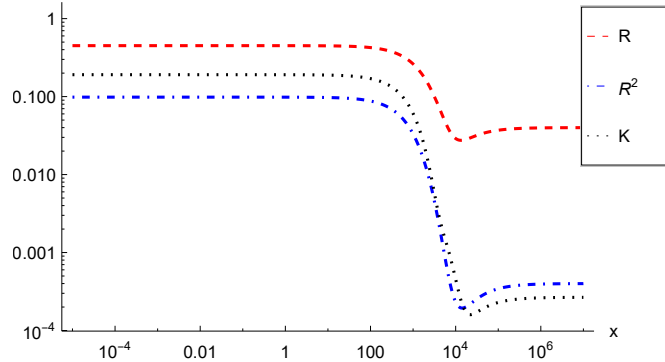


FIG. 5: The behaviour of curvature invariants for $M = 10^{10}$ and $\Lambda = 10^{-2}$.

$2GM \gg \ell_{Pl}$, $|\Lambda| \ll 12\pi/\Delta$, we obtain:

$$R^2 = \frac{144\pi^2}{\Delta^2} + \mathcal{O}\left[M^{-2/3}\right] \quad (5.17)$$

$$R_{\mu\nu}R^{\mu\nu} = \frac{72\pi^2}{\Delta^2} + \mathcal{O}\left[M^{-2/3}\right] \quad (5.18)$$

$$K = \frac{144\pi^2}{\Delta^2} + \mathcal{O}\left[M^{-2/3}\right]. \quad (5.19)$$

These expressions are valid for all four spacetimes considered in the previous subsection in the limit $2GM \gg \ell_{Pl}$, $|\Lambda| \ll 12\pi/\Delta$. We note that for macroscopic black holes, the curvature invariants attain a mass-independent limiting value fully determined by the area gap Δ , at the transition surface of the quantum bounce at $x = 0$ which replaces the singularity.

We now evaluate the curvature invariants in the asymptotic limit. Their asymptotic expressions in the limit $x \rightarrow \infty$ are given by

$$R^2 = 16\Lambda^2 + \mathcal{O}\left[\frac{1}{x}\right] \quad (5.20)$$

$$R_{\mu\nu}R^{\mu\nu} = 4\Lambda^2 + \mathcal{O}\left[\frac{1}{x}\right] \quad (5.21)$$

$$K = \frac{8\Lambda^2}{3} + \mathcal{O}\left[\frac{1}{x}\right]. \quad (5.22)$$

These asymptotic expressions are valid for all four possible spacetimes considered in the previous subsection based on the value of Λ . In particular, we note that the scalar curvature in the asymptotic limit is given by $R \approx 4\Lambda$. In case of ultramassive spacetimes with $\Lambda > 1/9G^2M^2$, the Plankian bound Λ_{max} determined by equation (4.3) helps in ensuring that the positive curvature is upper bounded in the asymptotic limit. Thus in case of ultramassive spacetimes, quantum effects may also appear in the asymptotic region. For the case of anti-deSitter spacetime with a central black hole, we have $\Lambda < 0$. The curvature in this case is negative and as discussed in the previous section, quantum gravity does not put any bounds on the negative curvature in this case. We are allowed to choose an arbitrarily large (and finite) negative value of the cosmological constant. However, it must be noted that the curvature still remains finite everywhere and the entire spacetime is regular as shown in the Penrose diagram in the Fig. 4. We show the behaviour of the

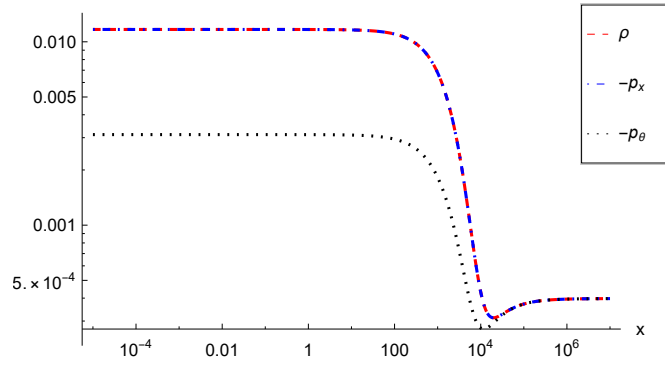


FIG. 6: The behaviour of energy density, radial pressure and tangential pressure for $M = 10^{10}$ and $\Lambda = 10^{-2}$.

curvature invariants for a small and positive Λ in Fig. 5. Since the effective metric is a symmetric function of x , the behavior of curvature invariants is also symmetric across the transition surface $x = 0$.

C. Effective stress-energy tensor

The effective stress-energy tensor provides an alternative viewpoint to understand the effects of quantum corrections. In this point of view, we consider the dynamics of the effective spacetime to be classical, i.e. governed by Einstein's equations, while the effects of quantum corrections manifest as a non-zero effective stress-energy tensor in an otherwise vacuum spacetime. The effective stress-energy tensor can be easily calculated from the effective metric as

$$T_{\mu\nu} = \frac{1}{8\pi G} G_{\mu\nu}, \quad (5.23)$$

where $G_{\mu\nu}$ is the Einstein tensor. From $T_{\mu\nu}$, we can readily extract the effective energy density ρ and the effective radial and tangential pressure densities p_x and p_θ respectively. In the region exterior to the black/white hole horizon, where the effective geometry has a time-like Killing vector (say X^μ), they are given by

$$\rho := \frac{T_{\mu\nu} X^\mu X^\nu}{(-X^\mu X_\mu)}, \quad (5.24)$$

$$p_x := \frac{T_{\mu\nu} r^\mu r^\nu}{r^\mu r_\mu}, \quad (5.25)$$

$$p_\theta := \frac{T_{\mu\nu} \theta^\mu \theta^\nu}{\theta^\mu \theta_\mu}. \quad (5.26)$$

where r^μ is a vector field pointing in the radial direction and θ^μ is a vector field pointing in the angular direction. In region bounded by black/white hole horizons, X^μ becomes space-like while r^μ becomes time-like, i.e. their roles get reversed. In the most quantum region at $x = 0$, in the limit $2GM \gg \ell_{Pl}$, $|\Lambda| \ll 12\pi/\Delta$, they attain a mass-independent limiting value determined by the

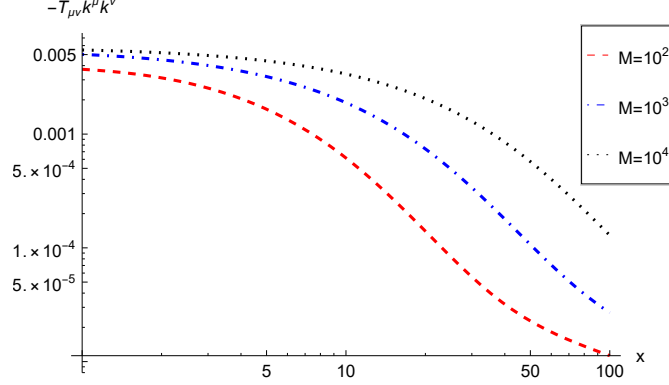


FIG. 7: Violation of the null energy condition for different values of black hole mass M .

area gap as follows:

$$\rho = \frac{1}{G\Delta} + \mathcal{O}\left[M^{-2/3}\right], \quad (5.27)$$

$$p_x = -\frac{1}{G\Delta} + \mathcal{O}\left[M^{-2/3}\right], \quad (5.28)$$

$$p_\theta = -\frac{1}{4G\Delta} + \mathcal{O}\left[M^{-2/3}\right]. \quad (5.29)$$

While their asymptotic behavior at spatial infinity is given by

$$\rho = \frac{\Lambda}{8\pi G} + \mathcal{O}\left[\frac{1}{x}\right], \quad (5.30)$$

$$p_x = -\frac{\Lambda}{8\pi G} + \mathcal{O}\left[\frac{1}{x}\right], \quad (5.31)$$

$$p_\theta = -\frac{\Lambda}{8\pi G} + \mathcal{O}\left[\frac{1}{x}\right], \quad (5.32)$$

showing that the effective spacetime is not asymptotically flat, just like its classical counterpart. We show the behaviour of the energy density and pressure in Fig. 6. As mentioned in the previous subsection, the behavior of energy density and pressures is symmetric across the transition surface $x = 0$, due to the symmetric nature of the effective metric.

Finally, note that in this subsection we are viewing the dynamics to be classical while the quantum corrections manifest as an effective stress-energy tensor. Therefore, for the singularity to be resolved, the null energy condition (NEC) must be violated as per the singularity theorems of Penrose & Hawking. To see this, we first change to a diagonal gauge by introducing the transformation

$$d\tilde{t} = dt + \frac{{}^{(0)}g_{tx}}{{}^{(0)}g_{tt}} dx. \quad (5.33)$$

In these coordinates, the metric is diagonal (denoted ${}^{(0)}\tilde{g}$), given by

$${}^{(0)}ds^2 = -f(x)d\tilde{t}^2 + \frac{\left(\sqrt{x^2 + \Delta^2/(x_0^{min})^2} + x_0^{min}\right)^2}{(x^2 + (x_0^{min})^2)f(x)} dx^2 + (x^2 + (x_0^{min})^2) d\Omega^2, \quad (5.34)$$

We expect NEC to be violated in the interior region, where the coordinate \tilde{t} becomes space-like (denoted by x_i in the interior) and x becomes time-like (denoted by \tilde{t}_i in the interior). It is now straight-forward to construct a null vector as

$$k^\mu = \frac{1}{\sqrt{-2 \, {}^{(0)}\tilde{g}_{\tilde{t}_i\tilde{t}_i} \, {}^{(0)}\tilde{g}_{x_i x_i}}} \left(\sqrt{{}^{(0)}\tilde{g}_{\tilde{t}_i\tilde{t}_i}} \tilde{X}^\mu + \sqrt{{}^{(0)}\tilde{g}_{x_i x_i}} \tilde{r}^\mu \right), \quad (5.35)$$

where \tilde{X}^μ is a space-like vector field in the interior and \tilde{r}^μ is a time-like vector field normal to the space-like hypersurfaces in the diagonal gauge. We then compute $T_{\mu\nu} k^\mu k^\nu$. The result is shown in Fig. 7 for three different black hole masses. We see that NEC is violated, indicating an avoidance of the singularity in accordance with the singularity theorems. We note that similar plots for NEC violation are obtained near the transition surface for all four distinct spacetimes considered above based on the value of Λ . As per the viewpoint of this subsection, the dynamics of the effective geometry is classical and singularity is resolved due to the violation of the NEC by the effective stress-energy tensor. Alternatively, from the point of view of loop quantum gravity, while the spacetime is vacuum, the quantum corrections are introduced in the geometry itself, which leads to the resolution of the singularity.

VI. CONCLUSIONS

In this manuscript, we have extended the spherically symmetric midisuperspace framework of loop quantum gravity using improved dynamics scheme to spherically symmetric black holes with a non-vanishing cosmological constant Λ , where Λ is allowed to range over both positive and negative values. This provides an interesting study of loop quantized black holes in spacetimes that are not asymptotically flat. Our quantization leads to a consistency condition which puts an Planckian upper bound on the possible values of a positive Λ which confirms the intuition gained from the analysis of homogeneous spacetimes with a positive Λ where a similar bound was obtained. Using semiclassical physical states, we obtained the effective metric which incorporates the lowest order quantum corrections. The effective metric is found to be manifestly regular, the singularity having been replaced by a transition surface, beyond which the spacetime can be extended. We show the causal structure of the spacetimes in four distinct cases depending on the value of Λ , including the case where the spacetime is asymptotically anti-deSitter. The effective spacetime is seen to possess various desirable features - (i) quantum effects modify the spacetime only in regions of high curvature inside the black hole horizon, (ii) the Planckian upper bound on Λ ensures that the curvature in asymptotic region does not exceed Planckian values, (iii) for macroscopic black holes, the curvature invariants approach a mass-dependent upper bound at the transition surface which replaces the singularity, (iv) the spacetime is regular at the transition surface which connects the trapped region inside the black hole horizon to an anti-trapped region on the other side, and (v) analysis of effective stress-energy tensor shows violation of null energy condition in the vicinity of the transition surface. A complete picture of the properties of these spacetimes can be obtained by a detailed study of the phenomenological aspects in future.

Appendix A: Quantization: Dynamics

The abelianization of the Hamiltonian constraint allows us to complete the Dirac quantization in our study. The steps we follow to find the solutions to the Hamiltonian constraint closely follow those of [16]. We will now promote the Hamiltonian constraint to a quantum operator acting on

the kinematical Hilbert space described in section III. Starting from the following expression for the Hamiltonian constraint:

$$H(\underline{N}) = \int dx \underline{N} \left(2E^\varphi \sqrt{\sqrt{|E^x|}(1 + K_\varphi^2) - 2GM - E^x \sqrt{|E^x|} \frac{\Lambda}{3}} - (E^x)'(|E^x|)^{1/4} \right). \quad (\text{A1})$$

we first absorb a factor of $|E^x|^{1/4}$ in the definition of the lapse so we are left with the simpler expression

$$H(\underline{N}) = \int dx \underline{N} \left(2E^\varphi \sqrt{(1 + K_\varphi^2) - \frac{2GM}{\sqrt{|E^x|}} - |E^x| \frac{\Lambda}{3}} - (E^x)' \right). \quad (\text{A2})$$

We now promote this quantity to a quantum operator by choosing an appropriate ordering:

$$\hat{H}(\underline{N}) = \int dx \underline{N} \left(2 \left[\sqrt{\left(1 + \frac{\sin^2(\widehat{\bar{\rho}}_j K_\varphi(x_j))}{\bar{\rho}_j^2} \right) - \frac{2GM\hat{M}}{\sqrt{\hat{E}^x}} - \hat{E}^x \frac{\Lambda}{3}} \right] \hat{E}^\varphi - (\hat{E}^x)' \right). \quad (\text{A3})$$

where we have performed the following substitution

$$K_\varphi \rightarrow \frac{\sin(\bar{\rho}_j K_\varphi(x_j))}{\bar{\rho}_j} \quad (\text{A4})$$

in order to have a well defined operator on the kinematical Hilbert space. We should in principle look for states $|\psi\rangle$ which are linear combinations of the spin network states $|\vec{k}, \vec{\mu}, M\rangle$ and are annihilated by the Hamiltonian constraint, that is, $\hat{H}(\underline{N})|\psi\rangle = 0$. We begin by noting that this operator acts only on the vertices of the spin network which can be easily seen from the action of the operator \hat{E}^φ given in (3.2) and from the fact that the action of $(\hat{E}^x)'$ on a spin network state $|\vec{k}, \vec{\mu}, M\rangle$ is proportional to the difference of the eigenvalues $\ell_P^2 k_j$ corresponding to two different points along the edge, therefore having a non zero contribution only at the vertices of the graph. With this in mind, we can write the Hamiltonian as a sum of operators acting on each vertex of the spin network.

$$\hat{H}(\underline{N}) = \sum_{v_j} \hat{H}(v_j) \quad (\text{A5})$$

We will now perform a change of representation first. Instead of using the holonomy representation for K_φ , it is more convenient to use the connection representation; the reason for this is that in the holonomy representation, the operator $\sin(\bar{\rho}_j K_\varphi(x_j))$ introduces a shift in the eigenvalues μ , resulting in a finite difference equation that is not possible to solve in closed form. Instead, if we adopt the connection representation for K_φ , the operator $\sin(\widehat{\bar{\rho}}_j K_\varphi(x_j))$ acts multiplicatively, while the action of \hat{E}^φ is simply $-i\ell_P \partial / \partial K_\varphi$. We are now ready to find the solutions to the Hamiltonian constraint, that is, states of the form

$$|\Psi\rangle = \int dM \prod_{v_j} \int_0^{\pi/\bar{\rho}_j} dK_\varphi(v_j) \times \sum_{\vec{k}} \psi(M, \vec{k}, \vec{K}_\varphi) |M, \vec{k}, \vec{K}_\varphi\rangle. \quad (\text{A6})$$

which are annihilated by (A5). Given that the Hamiltonian can be written as a sum of operators which act on different vertices, we may write

$$\psi(M, Q, \vec{k}, \vec{K}_\varphi) = \prod_j \psi_j(M, k_j, k_{j-1}, K_\varphi(v_j)). \quad (\text{A7})$$

Considering now a state of the form (A6), with the coefficients $\psi(M, \vec{k}, \vec{K}_\varphi)$ given by (A7), and recalling the action of \hat{E}^x given by (3.1), acting with the Hamiltonian constraint on such a state yields

$$4i\ell_P^2 \frac{\sqrt{1 + m_j^2 \sin^2(y_j)}}{m_j} \partial_{y_j} \psi_j + \ell_P^2 (k_j - k_{j-1}) \psi_j = 0, \quad (\text{A8})$$

where we have defined

$$y_j = \bar{\rho}_j K_\varphi(v_j),$$

$$m_j^2 = \bar{\rho}_j \left(1 - \frac{2GM}{\sqrt{\ell_P^2 k_j}} - \ell_P^2 k_j \frac{\Lambda}{3} \right),$$

Equation (A8) can be readily solved for ψ_j :

$$\psi_j(M, k_j, k_{j-1}, K_\varphi(v_j)) = \exp \left\{ \left(\frac{i}{4} m_j (k_j - k_{j-1}) F(\bar{\rho}_j K_\varphi(v_j), i m_j) \right) \right\} \quad (\text{A9})$$

where F is a two variable function defined by

$$F(A, B) = \int_0^A \frac{dt}{\sqrt{1 + B^2 \sin^2(t)}} \quad (\text{A10})$$

Physical states will then be given by

$$|\chi\rangle_{phys} = \int dM |M\rangle \bigotimes_j \left(\sum_{k_j} \chi(k_j) \psi_j(M, k_j, K_{\varphi,j}) |k_j\rangle \right), \quad (\text{A11})$$

Where the $\chi(k_j)$ are arbitrary functions of norm one on the kinematical Hilbert space. It can be verified that regardless of whether the m_j are real or imaginary, the ψ_j are either pure phases or bounded numbers [9], so that the solutions of the Hamiltonian constraint are well defined everywhere. Diffeomorphism invariance can be achieved by applying the usual group averaging procedure.

Then, a complete set of observables is given by the mass \hat{M} and the sequence of eigenvalues k_j . The later are typically written in a compact form as \hat{O}_z with eigenvalues $\ell_{\text{Pl}}^2 k_{\text{Int}(Sz)}$, with z being a parameter $z \in [-1, 1]$ such that the label j of any edge/vertex is given by $j(z) = \text{Int}(Sz)$, with S the total number of vertices in the spin network. Despite z is a continuous variable, its relation with j makes the collection of observables \hat{O}_z being finite, in agreement with k_j .

Therefore, in the kinematical Hilbert space there is a basis of states given by

$$\langle \vec{k}, M | \vec{k}', M' \rangle = \delta_{\vec{k}\vec{k}'} \delta(M - M'). \quad (\text{A12})$$

[1] A. Ashtekar, J. Olmedo & P. Singh, *Regular black holes from loop quantum gravity*, in *Regular Black Holes: Towards a New Paradigm of Gravitational Collapse* (pp. 235-282). Singapore: Springer Nature Singapore, (2023).

- [2] V. Husain, J. G. Kelly, R. Santacruz & E. Wilson-Ewing, *Fate of quantum black holes*, Physical Review D, 106(2), 024014, (2022).
- [3] K. Giesel, H. Liu, E. Rullit, P. Singh & S. Weigl, *Embedding generalized LTB models in polymerized spherically symmetric spacetimes*, arXiv:2308.10949 (2023).
- [4] I. Bengtsson, *A new phase for general relativity?*, Classical and Quantum Gravity, 7(1), 27 (1990).
- [5] T. Thiemann & H. A. Kastrup, *Canonical quantization of spherically symmetric gravity in Ashtekar's self-dual representation*, Nuclear Physics B, 399(1), 211-258 (1993).
- [6] M. Bojowald & H. A. Kastrup, *Symmetry reduction for quantized diffeomorphism-invariant theories of connections*, Classical and Quantum Gravity, 17(15), 3009 (2000).
- [7] R. Gambini & J. Pullin, *Loop quantization of the Schwarzschild black hole*, Physical review letters, 110(21), 211301 (2013).
- [8] M. Campiglia, R. Gambini & J. Pullin, *Loop quantization of spherically symmetric midi-superspaces*, Classical and Quantum Gravity, 24(14), 3649 (2007).
- [9] R. Gambini, J. Olmedo & J. Pullin, *Quantum black holes in loop quantum gravity*, Classical and Quantum Gravity, 31(9), 095009 (2014).
- [10] K. V. Kuchar, *Geometrodynamics of Schwarzschild black holes*, Physical Review D, 50(6), 3961 (1994).
- [11] M. Bojowald, *Spherically symmetric quantum geometry: states and basic operators*, Classical and Quantum Gravity, 21(15), 3733 (2004).
- [12] G. Oliveira-Neto, *Quantum mechanics of the Schwarzschild-deSitter black hole*, Physical Review D, 58, 024010 (1998).
- [13] M. Bojowald & R. Swiderski, *Spherically symmetric quantum geometry: Hamiltonian constraint*, Classical and Quantum Gravity, 23(6), 2129 (2006).
- [14] R. Gambini, J. Olmedo & J. Pullin, *Smooth extensions of black holes in loop quantum gravity*, International Journal of Modern Physics D, 32(16), 2350101 (2023).
- [15] R. Gambini, E. M. Capurro & J. Pullin, *Quantum spacetime of a charged black hole*, Physical Review D, 91(8), 084006 (2015).
- [16] F. Benítez, E. Mato & J. Olmedo, *Analysis of improved dynamics of nonrotating charged black holes*, Physical Review D, 109(6), 064011 (2024).
- [17] D. Martín de Blas, J. Olmedo & T. Pawłowski, *Loop quantization of the Gowdy model with local rotational symmetry*, Physical Review D 96, 106016 (2017).
- [18] D. W. Chiou, W. T. Ni & A. Tang, *Loop quantization of spherically symmetric midisuperspaces and loop quantum geometry of the maximally extended Schwarzschild spacetime*, arXiv:1212.1265, (2012).
- [19] R. Gambini, J. Olmedo & J. Pullin, *Spherically symmetric loop quantum gravity: analysis of improved dynamics*, Classical and Quantum Gravity, 37(20), 205012 (2020).
- [20] R. Gambini, J. Olmedo & J. Pullin, *Loop quantum black hole extensions within the improved dynamics*, Frontiers in Astronomy and Space Sciences, 8, 647241 (2021).
- [21] C. Rovelli, *Quantum Gravity*, Cambridge University Press (2007).
- [22] T. Thiemann, *Modern Canonical Quantum General Relativity*, Cambridge University Press (2007).
- [23] A. Ashtekar & J. Lewandowski, *Background independent quantum gravity: A Status report*, Classical & Quantum Gravity 21, R53 (2004).
- [24] W. Kaminski & T. Pawłowski, *The LQC evolution operator of FRW universe with positive cosmological constant*, Physical Review D 81, 024014 (2010).
- [25] T. Pawłowski & A. Ashtekar, *Positive cosmological constant in loop quantum cosmology*, Physical Review D 85, 064001 (2012).
- [26] E. Bentivegna & T. Pawłowski, *Anti-deSitter universe dynamics in LQC*, Physical Review D 77, 124025 (2008).